The role of colloids and other fractions in the below-ground delivery of phosphorus from agricultural hillslopes to streams

Catena 208 (2022) 105735

Contents lists available at ScienceDirect

Catena

journal homepage: www.elsevier.com/locate/catena

The role of colloids and other fractions in the below-ground delivery of phosphorus from agricultural hillslopes to streams

Maëlle Fresne [a,b,c,*], Phil Jordan [b], Karen Daly [c], Owen Fenton [c], Per-Erik Mellander [a,c]

[a] Agricultural Catchments Programme, Teagasc, Johnstown Castle Environment Research Centre, Wexford, Co. Wexford, Ireland
[b] School of Geography and Environmental Sciences, Ulster University, Coleraine, Northern Ireland, UK
[c] Crops, Environment and Land Use Programme, Teagasc, Johnstown Castle Environment Research Centre, Wexford, Co. Wexford, Ireland

ARTICLE INFO

Keywords:
Phosphorus
Colloids
Hillslope
Stream
Groundwater
Catchment

ABSTRACT

Colloids can be important for facilitated transfer of phosphorus (P) to groundwater (GW) and contribute to elevated P concentrations later delivered to surface water. To assess the role of colloidal P and other P fractions in delivery processes *via* below-ground pathways, this study investigated the influence of catchment and flow event characteristics on particulate (>450 nm), medium-sized colloidal (200–450 nm) and fine (<200 nm) P fractions in two agricultural hillslopes (TG, TA). Total and dissolved P fractions and their derivatives were also monitored. Samples in both stream and GW were taken weekly during baseflow conditions and every 2 h during storm conditions. Higher frequency monitoring of streamflow was also conducted to delineate hydrological flowpaths and determine P loads and hysteresis processes. Results indicated that during baseflow fine P was dominant in the streams (80 to 100 % of total P) and in shallow GW in TA (83 to 96 %) whereas in TG shallow GW was dominated by PP (55 to 96 %) possibly due to colloidal Fe-P complexes. Similarly, in TG shallow GW was dominated by PP (79 to 81 %) during high flow events. During a larger flow event (within the period of land fertilization) the quickflow pathway (24 % of total flow) delivered 3.2 g ha^{-1} of PP which was dominant in the stream (44 to 68 %). A smaller flow event (within the period of prohibited land fertilization) facilitated delivery of P *via* deeper baseflow pathways (87 % of total flow) as fine reactive P (1.3 g ha^{-1}), also dominant in the stream (73 to 78 %). The research indicated a very limited presence of medium-sized colloidal P but a large presence of fine P that may contribute to elevating P concentrations above environmental thresholds. Further work should constrain the controlling factors for colloidal P presence/absence and also on the extent and speciation of coarser and finer fractions in the hillslope to stream continuum.

1. Introduction

Phosphorus (P) is a key nutrient for plant growth and food security (Cordell and White, 2014) but it can also be lost from agricultural land and contributes to the eutrophication of water bodies (Withers et al., 2014). This is a continuing global problem (Sinha et al., 2017) and a challenge for achieving water quality targets. In many countries, for example, the principal issue in trying to achieve good ecological status is an excess of nutrients from terrestrial sources (Sharpley et al., 2000; Schoumans et al., 2014; Sinha et al., 2017).

For the most part, research and mitigation measures for P have focused on above ground hydrological pathways (Doody et al., 2012; Moloney et al., 2020) and there has been little focus on below-ground P delivery to surface water (Holman et al., 2008; McDowell et al., 2015). However, subsurface pathways can contribute to maintained P delivery to surface water over the year including summer periods of high eutrophication and ecological risk (Shore et al., 2017).

Concentrations of P in GW are influenced by soil chemical and physical properties such as aluminium (Al) and iron (Fe) content (Lookman et al., 1995; Mellander et al., 2016), pH and clay content (Mabilde et al., 2017) or macropores and preferential flowpaths (Bol et al., 2016; Julich et al., 2017). Other influences include bedrock P (sediments) and dissolution of P-rich minerals (McGinley et al., 2016) and GW P concentrations can therefore vary in space. Temporal variations have been related to GW depth (Mabilde et al., 2017) and P release from Fe-oxide reductive dissolution (Dupas et al., 2015; Neidhardt et al., 2018). Moreover, hydrological dynamics of hillslope shallow subsurface flows are highly variable in both space and time (Bachmair et al., 2012)

* Corresponding author at: Agricultural Catchments Programme, Teagasc, Johnstown Castle Environment Research Centre, Wexford, Co. Wexford, Ireland.
E-mail address: maelle.fresne@hotmail.fr (M. Fresne).

https://doi.org/10.1016/j.catena.2021.105735
Received 18 May 2021; Received in revised form 25 August 2021; Accepted 13 September 2021
Available online 24 September 2021

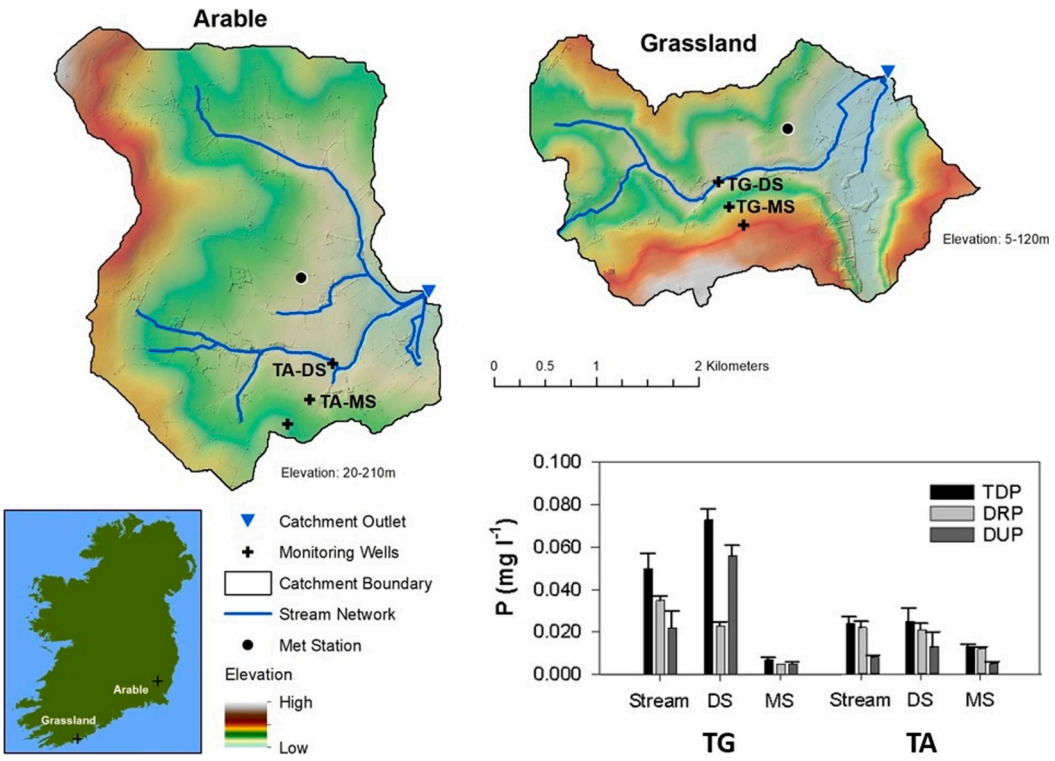

Fig. 1. Location of the two study catchments in Ireland and instrumentation with study hillslopes and transects (T). For reference, the graph shows average concentrations (± standard error; only bars in the positive direction are shown) of total dissolved P (TDP), dissolved reactive P (DRP) and dissolved unreactive P (DUP) in stream and shallow GW (monthly grab samples, 2010–2017 – unpublished ACP data). MS and DS denote midslope and downslope, respectively.

and can influence GW P loads delivered to surface water. Controlling factors include rainfall (Duan et al., 2017; Lehmann et al., 2007), soil topography (Bachmair and Weiler, 2012) and/or preferential flowpaths (Anderson et al., 2009) as well as bedrock topography and permeability (Tromp-van Meerveld and Weiler, 2008; Graham et al., 2010). Consequently, inter-storm event variability can be observed in the quantity and speciation of P to event climatic drivers and pre-event soil conditions (Van Esbroeck et al., 2017) as well as to P sources and seasonality (Bender et al., 2018). Therefore, despite attenuation processes (adsorption) occurring in the subsurface soil and bedrock (Neidhardt et al., 2018), GW P contribution to stream P can be a concern (Mellander et al., 2016). This can be indicated by a higher contribution of bioavailable P (to total P (TP)) associated with a greater proportion of baseflow in rivers (Schilling et al., 2017) and P concentration pressures greater during baseflow than during stormflow (Shore et al., 2017).

Most surface water and GW monitoring campaigns focus on the total and dissolved (<450 nm) P fractions, but recent stream monitoring research has included highly mobile colloidal P fractions. For example, colloidal P in fractions from 1 nm to 1000 nm have been found to represent 30 % of stream total dissolved P (TDP) by Gu et al. (2020) and up to 100 % of TP by Gottselig et al. (2014) with stream P dominantly bound to Fe-rich colloids (Baken et al., 2016b). However, in these studies monitoring of colloidal P was carried on a limited frequency and time window and with no consideration of the role of GW. Hence, as below-ground flowpaths can contribute to substantial P delivery to streams in GW driven catchments, leading to elevated P concentrations throughout the year, an assessment of the role of GW colloidal P in P delivery processes is required. This is especially relevant as colloidal P appears to be a much more significant contributor to P losses from agricultural lands in some landscapes (forested, riparian wetland and arable areas) than previously assumed (Gottselig et al., 2014; Gu et al., 2020; Jiang et al., 2015), and is a potentially bioavailable P form (Montalvo et al., 2015).

A better understanding of how landscape properties control the spatio-temporal occurrence and intensity of colloidal P delivery is also required to better evaluate and quantify processes controlling P transfers in catchments and subsequently better target mitigation measures to minimise P losses. In particular, the role of soil chemical and physical properties in controlling colloidal P sources, mobilisation and concentrations in soil solution is of concern (Henderson et al., 2012; Ilg et al., 2008; Jiang et al., 2013; Mohanty et al., 2015; Siemens et al., 2004; Fresne et al, 2021). Additionally, the process of colloidal P transfer through the soil profile and unsaturated zone (USZ) to GW is not widely assessed in the field. Agricultural land and fertilization management are also known to control colloidal P processes (Heathwaite et al., 2005; Schelde et al., 2006). Moreover, as the quantity and speciation of P varies with storm events (Bender et al., 2018; Van Esbroeck et al., 2017), understanding how the interaction of these landscape structures with climatic variables control colloidal P dynamics in GW and surface water is required. This would provide better evaluations of the inter-annual occurrence and intensity of colloidal P delivery and the effect of climate change on colloidal P processes. The knowledge gap here is related to colloidal P transfers from hillslope GW to adjacent surface waters in agricultural catchments.

Therefore, the aim of the present study was to investigate pathway dynamics and the below-ground delivery of P. For this a hillslope to stream experiment was established to separate out the 450 nm threshold so that colloidal P could be considered. The experiment considered P species either side of this threshold with the intention to isolate the medium-sized colloidal P species more particularly between 450 nm and 200 nm in a first campaign. Previous batch scale work had suggested this medium-sized colloidal P fraction had a role in P mobilised from Irish soils but with the extent determined by soil chemical properties and fertilizer type (Fresne et al., 2021). As a follow on from this work, the objectives in this study were to examine the role of colloidal P and other P fractions delivered to surface water *via* below-ground pathways in catchment hillslopes to streams:

Table 1
Transect soil and lithology characteristics.

Transect	Location	Soil type[a]	Soil texture[b]	TP[b] (mg kg^{-1} soil)	M3-P[b] (mg kg^{-1} soil)	M3-Fe[b] (mg kg^{-1} soil)	M3-Al[b] (mg kg^{-1} soil)	DPS[b] (%)	Hillslope zone – Geological zone – Screen depth[c]	Bedrock hydraulic conductivity[d] (m d^{-1})
TG	DS	Gleysol	Sandy Loam	602	90	261	818	8.3	Near stream, shallow – Weathered rock – 4–7 m	0.5
	MS	Cambisol/ Podzol	Loam	635	45	349	791	4.0	Upland, shallow – Bedrock – 10.5–13.5 m	2.8
TA	DS	Luvisol	Loam	1042	131	300	978	10.2	Near stream, shallow – Transition zone – 3.5–6.5 m	4.2
	MS	Cambisol	Loam	1010	56	171	1034	4.6	Upland, shallow – Weathered rock – 6–9 m	4.2

[a] World Reference Base classification
[b] soil tests on composite soil samples (0–40 cm) taken in January 2018 in the study locations (from Fresne et al., 2021). TP: total P; M3-P: Mehlich 3 extractable P; M3-Fe: Mehlich 3 extractable iron; M3-Al: Mehlich 3 extractable aluminium; DPS: degree of P saturation
[c] from Mellander et al. (2014)
[d] from McAleer et al. (2016)

1) with contrasting dominating soil chemistry and land use;
2) during contrasting (duration, total rainfall, seasonality) rainfall events.

2. Materials and methods

2.1. Catchment descriptions

Two catchment observatories in Ireland were used for this study as part of the long-term Agricultural Catchment Programme (ACP) (Fealy et al., 2010; Wall et al., 2012): 'Grassland A' (7.6 km^2) and 'Arable A' (11.2 km^2) (Fig. 1) named hereafter 'Grassland' and 'Arable'. The two catchments have groundwater-fed streams but contrasting land use and stream outlet P concentrations (Mellander et al., 2016). Grassland has mainly intensively managed grassland farms (dairy and beef) with soils dominated by well drained Brown Earths (Cambisol) and Brown Podzols (Podzol) (84 %). The bedrock is Devonian old red sandstone, mudstone and minor siltstone and is classified as a productive aquifer. Hydrological pathways are mostly below ground within the shallow weathered bedrock. Arable has predominantly arable crop production (spring barley) with soils dominated by well drained Brown Earth (Cambisol) (80 %). The bedrock is Ordovician volcanic slate and silt-stone and is poorly productive with fissure-flow within the stratified zones of highly permeable weathered rock (Mellander et al., 2012).

2.2. Experimental set-up

In the centre of each catchment a weather station (Campbell Scientific Base Weather Station, Fig. 1) monitored rainfall and standard meteorological parameters at a 10-minute resolution. Stream discharge at the outlets of each catchment was calculated *via* rating curves on flat-v weirs developed using area-velocity measurements (OTT Acoustic Doppler Current-meters) and water level measurement with vented-pressure instruments (OTT Orpheus Mini) on a 10-minute basis

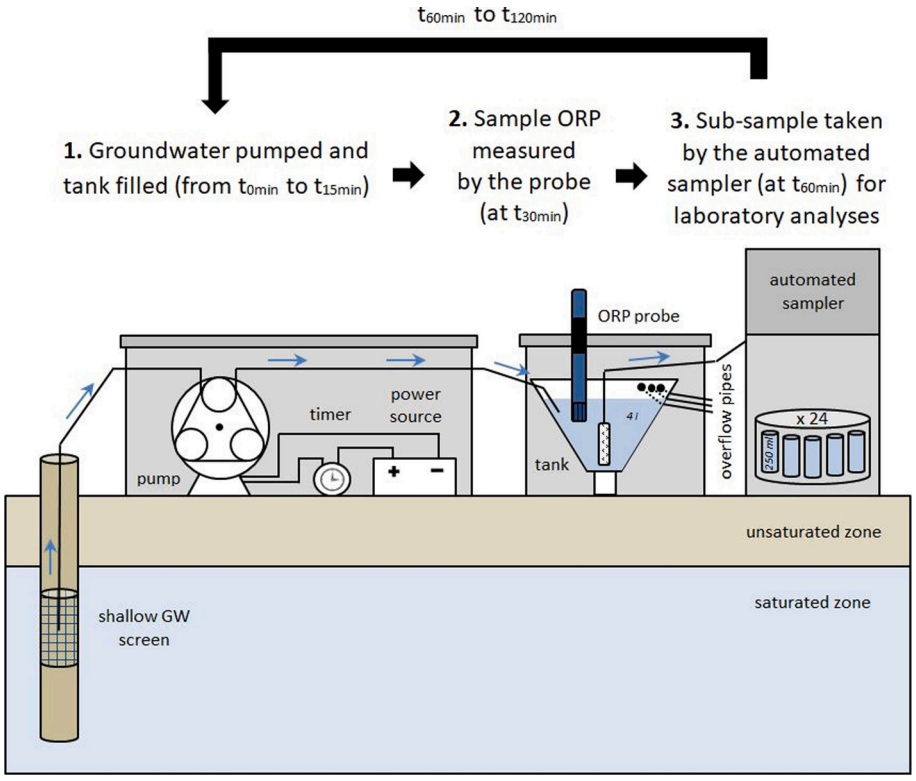

Fig. 2. Schematic of the automated low-flow and low-disturbance GW sampler which operated on a 120 min cycle described as follows: 1) GW is pumped for 15 min (from t_{0min} to t_{15min}) from the piezometer, the tank is filled; 2) the multiparameter probe installed in the tank measures sample oxidation reduction potential (ORP) 15 min later (at t_{30min}); 3) the automated sampler installed in the tank takes a sub-sample 30 min later (at t_{60min}). The pumping of the next sample starts 60 min later (at t_{120min}) and the same cycle starts again.

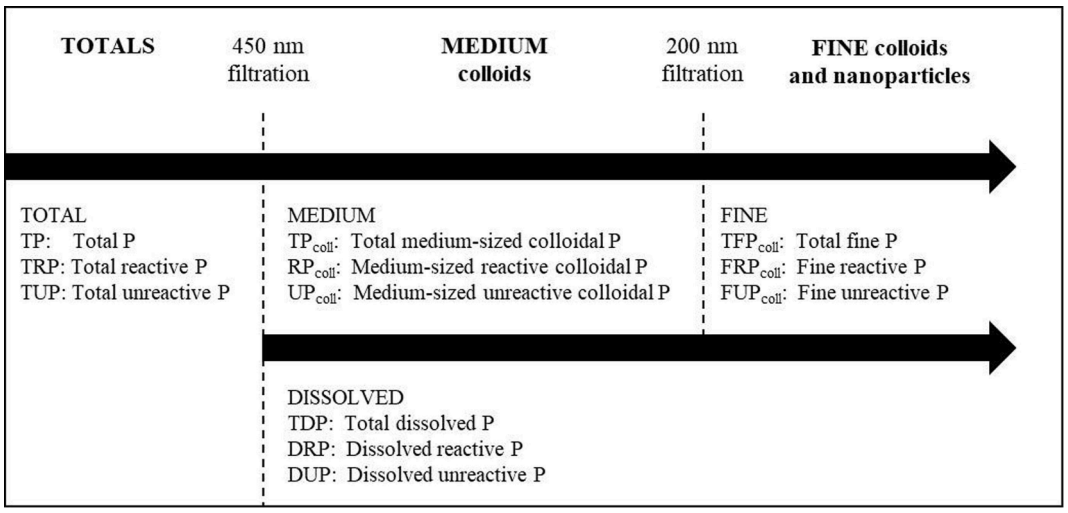

Fig. 3. Terminology used for the different operational/colloidal P fractions and species.

(Mellander et al., 2016). Total P and total reactive P concentrations were measured concurrently with stream discharge using bankside analysers (Hach Phosphax Sigma), used here to characterise storm events.

In each catchment as part of the ACP there are monitoring wells along hillslope transects with screens sampling the shallow GW (described in detail in Mellander et al. (2014) and McAleer et al. (2017)) downslope near the stream channel (DS) and midslope (MS) to investigate below-ground nutrient transfer pathways. Transects TG (Grassland) and TA (Arable) were used for this study as they have previously indicated relationships with contrasting stream P concentrations (Mellander et al., 2016) and different P fractions in shallow GW (Fig. 1). Transect soil and lithology characteristics are shown in Table 1.

In addition to this long-term monitoring instrumentation, mini lysimeters (Dupas et al., 2015) were installed in triplicate at DS and MS sites on the TG and TA transects to capture free soil solution in the USZ at a depth of 40 cm (**Appendix Figure A**). This was to determine baseline soil water P concentrations potentially influenced by site static characteristics (soil, subsoil), in relation to previous findings by Fresne et al. (2021) on the influence of soil chemistry on medium-sized colloidal P.

Near-stream (DS) monitoring wells on the TG and TA transects were set-up with additional equipment to capture chemistry changes during storm events. The shallow GW was automatically sampled using a bespoke automated low-flow and low-disturbance GW sampler (Fig. 2). The system consisted of a pump connected to a timer, an intermediate 4 L tank and an automated sampler (ISCO 1612, Teledyne) and was started manually at the onset of storm rain. The pumping speed was set to less than the aquifer recharge rate and the pumped volume (from t_0 to t_{15min}) was three times the volume of the tank to insure a full replenishment of the tank and limit sample contamination with previous samples. The intermediate tank was also fitted with an EXO1 multi-parameter sonde (YSI), with Oxygen Redox Potential (ORP) data collected to further contextualise GW conditions.

In the streams adjacent to the DS points on the TG and TA transects, water level and flow velocity were recorded on a 5-minute basis using a Flowlink velocimeter (ISCO). Stream discharge was calculated on a 5-minute basis after determination of water level/wet area relationship resulting from stream cross-section measurements. Owing to a malfunction with the velocimeter at TG (**Figure B**), the adjacent stream (near TG-DS), and immediately after the Grassland catchment outlet, were manually gauged (OTT Acoustic Doppler Current-meters) during low and high flow occasions. The relationship upstream discharge-outlet discharge was used as a substitute to calculate discharge at TG from the outlet discharge records. In the streams, an EXO1 multi-parameter sonde (YSI) was also deployed to gather turbidity data (30-min resolution) during storm events to validate flow pathway delineations in a later analysis.

2.3. Baseline and storm sampling

To characterise P in the hillslope-stream continuum, baseline samples were taken from the soil solution , shallow GW and the adjacent stream. Stream water, and DS and MS soil solution and shallow GW sampling was carried out weekly. Stream samples were manually collected using a 500 ml Sarstedt polyethylene container. Groundwater samples were collected using a 200 ml double valve bailer (Solinst, Canada). Stream water and shallow GW ORP was measured *in situ* using an Aquaprobe AP-700/800 (Aquaread). For soil solution, samples were manually collected using a 100 ml BD Plastipak polypropylene syringe rinsed with deionized water between each sampling. No samples were collected when the soil was dry. All samples were stored in 500 ml Sarstedt polyethylene containers until filtration.

During storm rainfall events, stream water and near-stream shallow GW (DS) sampling was simultaneously carried out every 2 h at sites adjacent to the DS sites. Sampling frequency was chosen by examining the time of passage of historical stream outlet flow peak data to capture the whole event. Stream and GW samples were collected using the automated samplers (ISCO 1612, Teledyne) (24 × 500 ml sample bottles, automatically pre-rinsed tubing) that were started manually shortly before storm rain was forecast to begin. Samples were returned from the field within 24 h of the first sample being taken. After each sampling campaign, all sample bottles were dishwasher cleaned using a P free detergent, washed in an 11 % hydrochloric acid bath, and rinsed in two successive baths of deionized water.

Storms were contextualised according to antecedent daily soil moisture deficits (SMD) modelled for well-drained soils (Schulte et al., 2005) from weather stations data, and by the P fluxes in the streams using the measured P concentrations and discharge data at catchment outlets.

2.4. Phosphorus speciation and supporting data

Subsamples of the water samples were kept unfiltered or were filtered using two filter pore sizes (450 and 200 nm). Filtration was undertaken using cellulose acetate syringe filters (Sartorius) within 1 (baseline samples) to 3 (storm rainfall samples) hours after the samples were returned from the field. Raw and filtered samples were stored in cool boxes for transportation to the laboratory, then refrigerated at 4 °C prior to analysis. Total P species were determined on unfiltered, digested (alkaline persulphate oxidation (Askew, 2005) for the TP fraction) and undigested samples (for the total reactive P (TRP) fraction). Dissolved

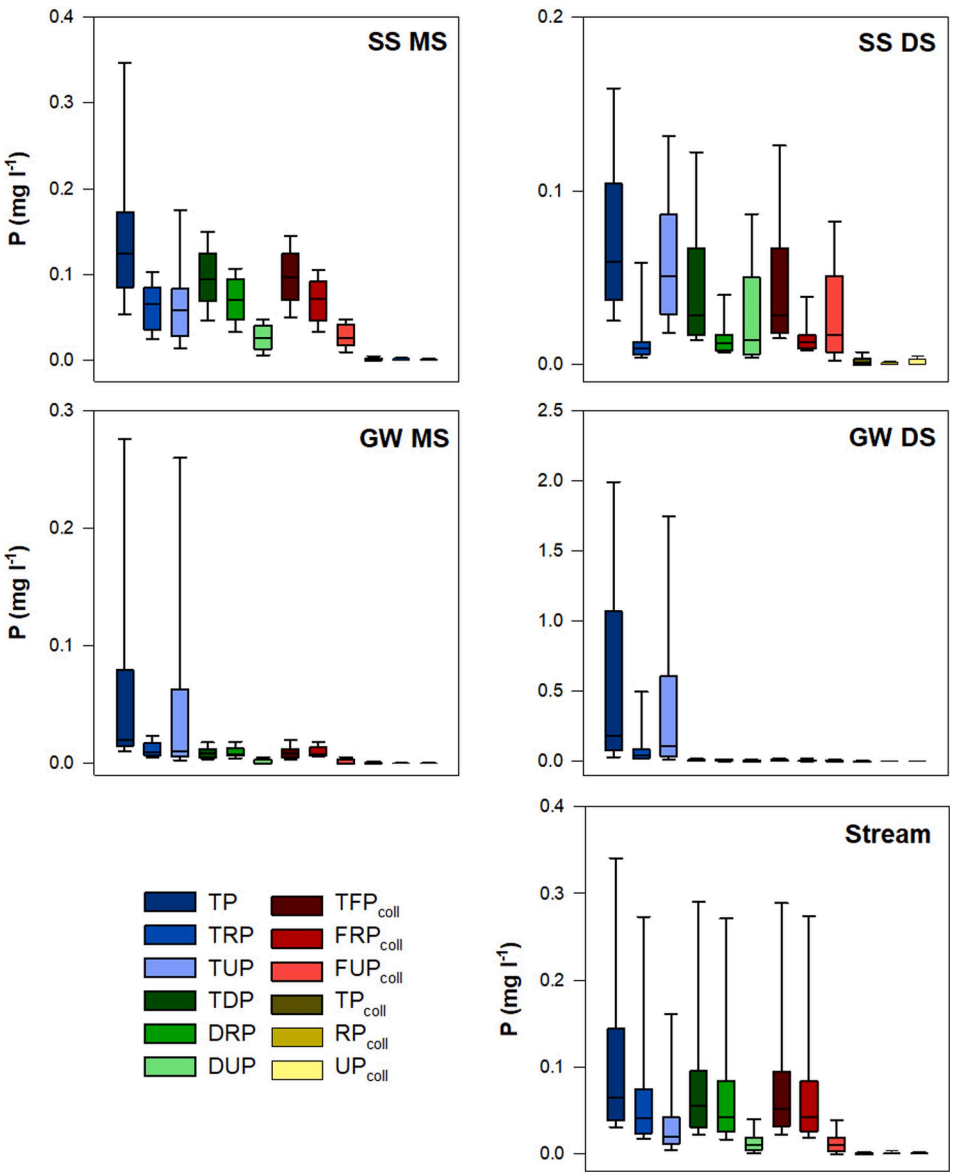

Fig. 4. Distribution of the concentrations of total (blue), dissolved (green), medium-sized colloidal (yellow) and fine (red) P fractions (total (dark colour), reactive and unreactive (light colour) P species) in the locations of transect TG over the baseline sampling period (August 2019-March 2020). SS denotes soil solution, GW denotes groundwater, DS denotes downslope and MS denotes midslope. (For interpretation of the references to colour in this figure legend, the reader is referred to the web version of this article.)

species were determined on filtered, digested and undigested samples. Phosphorus was determined by spectrophotometry after molybdate reaction and ascorbic acid reduction (method detection limit (MDL): 0.005 mg l^{-1}) (Askew and Smith, 2005a). A flow chart of all the P species is presented in Fig. 3.

In all filtered and unfiltered samples, the difference between a TP and a RP fraction was considered an unreactive P (UP) fraction. The 450 nm filtrates were considered as 'operationally dissolved' but also the upper boundary of medium-sized colloidal P species. The 200 nm filtrates were considered a pool of fine colloidal, nano-particulate, and truly dissolved P, defined here as fine P. The 200 nm filtrates were also considered as the lower boundary of medium-sized colloidal P species (adapted from Missong et al., 2018) (Fig. 3). In this way the difference between 'dissolved' 450 nm filtrates and 200 nm filtrates was considered the medium-sized colloidal P pool and species. Similarly, the difference between TP and total dissolved P (TDP) was considered particulate P (PP) whereby the particles were >450 nm and so therefore in the larger colloidal range (i.e. including up to 1000 nm and other larger particles).

The period of sampling coincided with normal land management that included fertilisation. A record of this is provided in **Table A**. Unfiltered samples were also analysed for iron (Fe) and aluminium (Al) using a Varian Vista-MPX CCD-Simultaneous ICP-OES (instrument detection limit (IDL): 1 μg l^{-1}) (Gottler and Piwoni, 2005), for organic carbon (OC) using a non-Diffractive Infra-Red (NDIR) detector after acidification and combustion (Baird, 2005), and for nitrate-nitrogen (NO_3^--N) calculated as the difference between total oxidised nitrogen (TON) determined by alkaline hydrazine reduction (MDL: 0.1 mg l^{-1}) (Askew and Smith, 2005b) and nitrite-nitrogen (NO_2^--N) determined by diazotisation (MDL: 0.006 mg l^{-1}) (Askew and Smith, 2005c).

2.5. Data processing

For each transect, negative concentrations in TP and RP (in the total, dissolved and fine fractions) within the MDL were replaced by zero concentrations. Negative concentrations below the MDL were discarded. Unreactive P concentrations were then calculated as the difference between TP and RP and negative concentrations were managed using the same procedure as for TP and RP. This procedure occurred when results were near or below the MDL and a similar procedure was undertaken for species calculated by difference in the medium-sized colloidal P species. Percentages of negative values, negative values replaced by zero and negative values discarded for all P species and fractions of transects TG

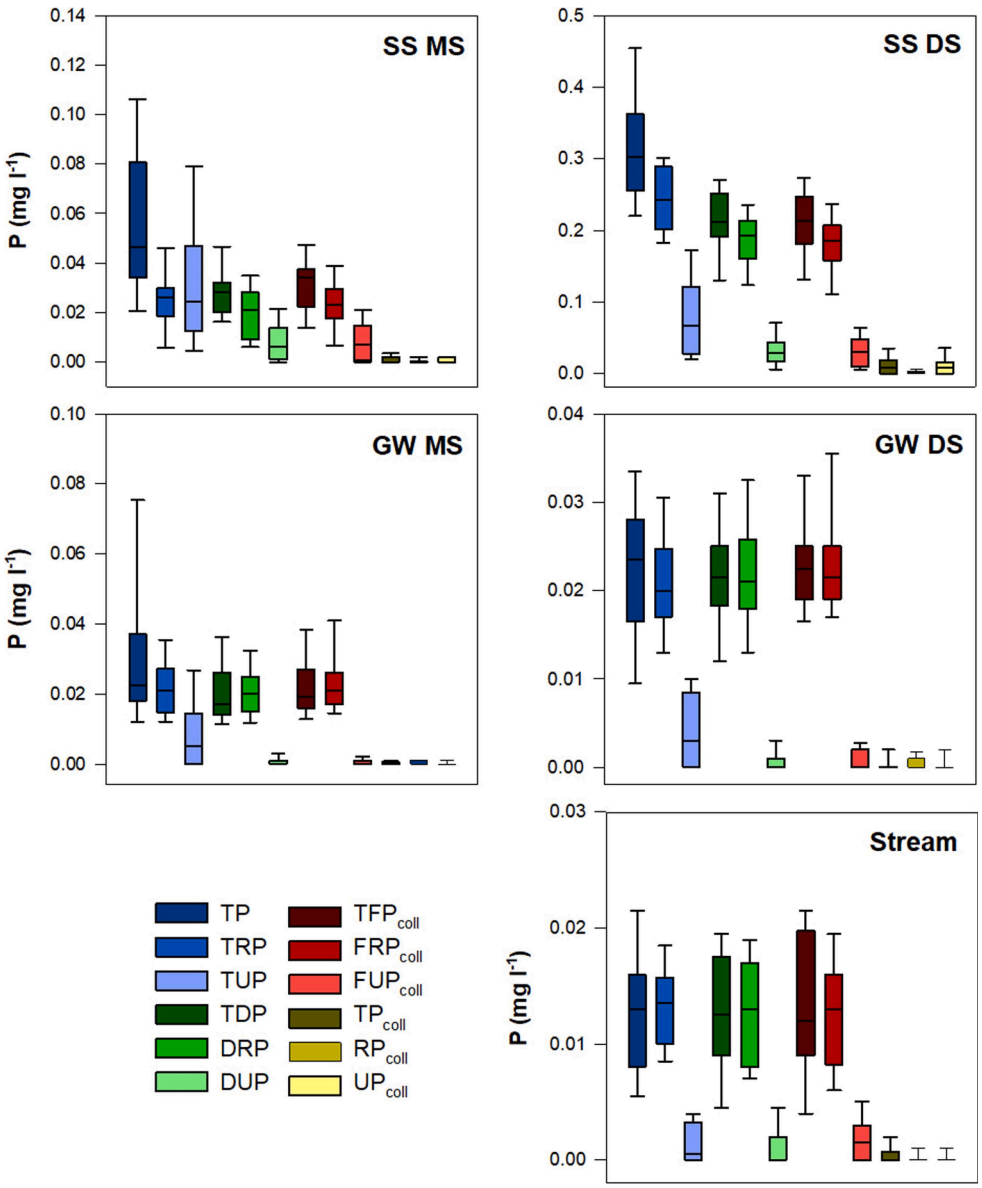

Fig. 5. Distribution of the concentrations of total (blue), dissolved (green), medium-sized colloidal (yellow) and fine (red) P fractions (total (dark colour), reactive and unreactive (light colour) P species) in the locations of transect TA over the baseline sampling period (February 2019-June 2019). SS denotes soil solution, GW denotes groundwater, DS denotes downslope and MS denotes midslope. (For interpretation of the references to colour in this figure legend, the reader is referred to the web version of this article.)

and TA are presented in **Table B**. Overall, 12 % of the results in TG and 18 % of the results in TA were processed in this way. The negative concentrations for the additional chemical parameters (i.e., Al, Fe, TOC, NO_3^--N) were handled using the same procedure.

The baseline physico-chemical time series were visualised for each location and Cook's D test (Cook, 1979) was performed to statistically localise and remove potential outliers (assumed when $D > 1$). Shapiro Wilk's normality tests were then performed for each P species, fraction, and location (as well as for each additional chemical parameter). Following these tests (data distributions were not normal), median and interquartile range were calculated for each measured parameter.

For storm rainfall events, measured stream P concentrations at TG and TA were synchronised with the adjacent total stream flow of the previous 2 h to calculate P loads delivered during these 2 h. Concentration-discharge (C-Q) hysteresis was also studied to reveal the size and mobility of the different P pools (e.g. Bieroza and Heathwaite, 2015). Flowpath separation was carried out on the hydrographs generated by the storms by visual assessment of the inflection points in the steepness of the event recession limb to delineate quickflow (QF, surface runoff, drain water and preferential flow), interflow (IF, soil water), shallow baseflow (SF, shallow GW) and deeper baseflow (BF, deeper GW) transfer pathways using the terminology for Irish catchments reviewed in Archbold et al. (2010). Each segment (between two inflection points) represents different dominant transfer pathways. Pathways were separated logarithmically from the start of the rising limb to the inflection point, assuming a logarithmic response in baseflow to the rainfall event. The hydrological transfer pathways were then verified using turbidity (elevated during QF – presented in **Figure C**, not verified during G-2 due to technical issues) using the method described by Mellander et al. (2012). The average P load for each measured fraction and species delivered *via* each pathway was calculated using the average P concentration and the total stream flow of each pathway. Measured GW ORP and P concentrations were synchronized with the time when GW pumping started, which coincided with the time when stream water was sampled.

3. Results

3.1. Colloidal phosphorus contribution to baseline phosphorus concentrations

Distributions of the concentrations of the different P fractions and

species in soil solution, shallow GW and stream along the two study transects TG and TA over the baseline sampling periods are shown in Fig. 4 and Fig. 5.

In TG-MS, soil solution P and shallow GW P were mainly FRP_{coll} and TUP whereas in TG-DS P was mostly TUP (using the terminology in Fig. 3) (Fig. 4). The fine P (<200 nm; fine colloidal, nano-particulate and truly dissolved P) fraction contributed to 45 % (based on the median value) of shallow GW TP at TG-MS and to 4 % at TG-DS. By comparison, PP (>450 nm; difference between total and dissolved fractions) accounted for 55 % and 96 % of shallow GW TP at TG-MS and TG-DS, respectively. TG-stream P concentrations were high (above the Environmental Quality Standard (EQS) of 35 μg l^{-1} of TRP) and P was dominantly FRP_{coll} (Fig. 4). This fine P fraction was dominant in TG-stream where it accounted for 80 % of TP (65 % as reactive P and 15 % as unreactive P). The medium-sized colloidal P fraction had a limited contribution (0–2 %) to TP in soil solution, shallow GW and in stream.

In TA-MS, soil solution P was mostly FRP_{coll} and TUP, and FRP_{coll} at TA-DS while shallow GW P was mostly FRP_{coll}. TA-stream P concentrations were lower than in TG and below the EQS with P dominantly FRP_{coll} (Fig. 5). The fine P fraction was dominant in shallow GW and TA-stream where it accounted for 83 % and 96 % of TP at TA-MS and TA-DS, respectively, and 100 % of TP in TA-stream (reactive P). The medium-sized colloidal P fraction did not appear to contribute to TP in shallow GW and in the stream and had a limited presence in soil solution at DS (3 % of TP).

3.2. Colloidal phosphorus contributions to flow event phosphorus dynamics

3.2.1. Storm events

Two storm events (G-1 and G-2) were monitored in the Grassland (TG) catchment which was a hotspot as suggested by the higher stream P concentrations and the higher proportion of DUP in stream and GW at DS (Fig. 1). One storm event (A-1) was monitored in the Arable (TA) catchment. Hydrometric and hydro-chemical characteristics of the flow events are presented in Table 2. Flow event G-1 had a long duration with low total rainfall, G-2 had a long duration with high total rainfall and A-1 had a short duration with low total rainfall. Soil moisture deficit before the event was low and comparable between G-1 and G-2, and higher before A-1. Event TP load was higher in TG than in TA especially during G-2.

3.2.2. Phosphorus in shallow groundwater and stream

During flow events in TG (G-1, G-2), stream P concentrations were up to ten times higher than those measured in TA (A-1). Fine P (TFP_{coll}) concentrations peaks were close or above the EQS (Figs. 7, 10, 11).

During G-1, shallow GW P was dominantly TUP (Fig. 6) with concentrations peaking at the same time as the first P peak in the stream where FRP_{coll} was dominant and two P peaks were observed (Fig. 6, Fig. 7). The BF pathway was dominant (87 % of the total flow) and transferred mostly FRP_{coll} (1.3 g ha^{-1}) (Fig. 8). The clockwise then anti-clockwise C-Q hysteresis (Fig. 9) suggested that a first P source was easily mobilised or proximal whereas a distant second P source was later connected (Evans and Davies, 1998; House and Warwick, 1998). In contrast, during G-2, shallow GW P was dominantly TUP as was stream P (Fig. 6, Fig. 10), especially when the QF pathway was dominant. Shallow GW P concentrations peaked at the same time as the second P peak in stream where two P peaks were observed (Fig. 10). Over the event, 66 % of the flow occurred as BF that transferred both FRP_{coll} (1.5 g ha^{-1}) and TUP (1.2 g ha^{-1}). Quickflow (QF) only transferred 24 % of the flow but delivered a high load of TUP (3.2 g ha^{-1}) (Fig. 8). The C-Q hysteresis showed that the two P sources were proximal or easily

Table 2
Hydrometric and hydro-chemical summary of the flow events monitored in the two study transects.

Transect	TG		TA
Name of flow event	G-1	G-2	A-1
Date of flow event	14-15th October 2019	8-10th February 2020	12th June2019
Duration rainfall event (h)	17	19	8
Total rainfall (mm)	11.6	28.6	6.4
Maximum rainfall intensity (mm h^{-1})	3.6	7.2	1.8
SMD day before event (mm)	0.0	2.2	25.2
Total discharge (m^3)	12 088	25 111	675
Total discharge (mm)	4	8	0.2
TP (g $ha^{-1}h^{-1}$)	0.126	0.339	0.003
TRP (g $ha^{-1}h^{-1}$) (% of TP)	0.094 (75)	0.102 (30)	0.002 (66)
TUP (g $ha^{-1}h^{-1}$) (% of TP)	0.032 (25)	0.237 (70)	0.001 (34)

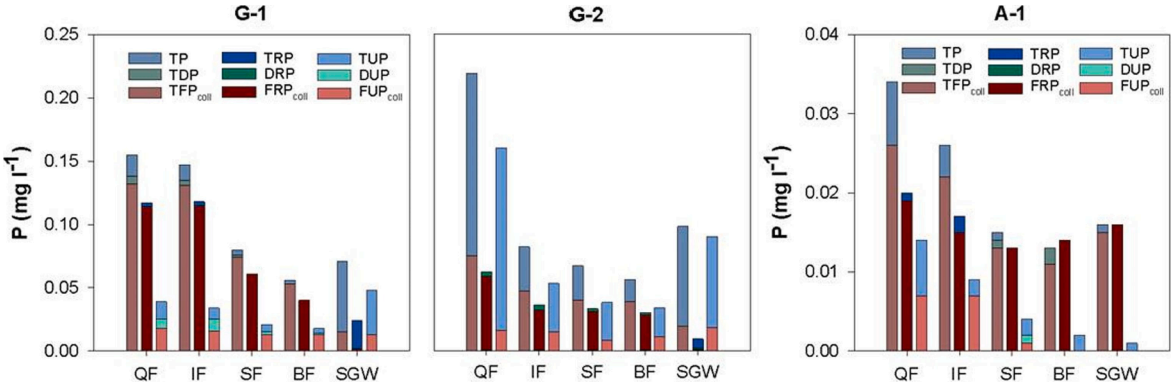

Fig. 6. Phosphorus flow weighted average concentrations in the streams during quickflow QF, interflow IF, shallow baseflow SF, deeper baseflow BF and in shallow GW (SGW) at DS during flow events G-1, G-2 and A-1. Fine P (red) is included in dissolved P (green) which is included in total P (blue). The difference between TDP and TFP_{coll} is TP_{coll}, the difference between DRP and FRP_{coll} is RP_{coll} and the difference between DUP and FUP_{coll} is UP_{coll}. (For interpretation of the references to colour in this figure legend, the reader is referred to the web version of this article.)

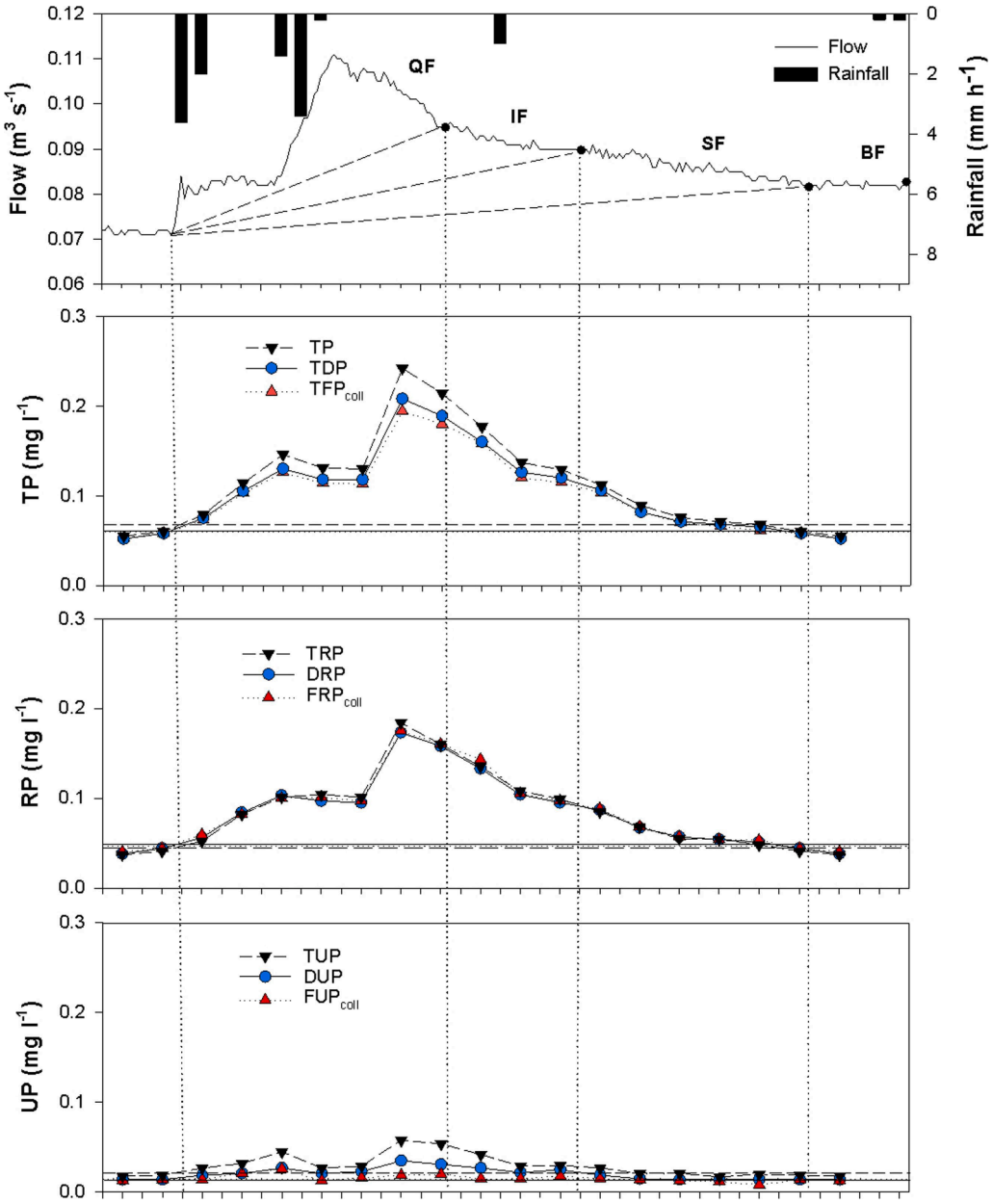

Fig. 7. Total P, reactive P and unreactive P (in the total, dissolved and fine P fractions) transfer pathways based on hydrograph recession analysis for flow event G-1. QF, quickflow; IF, interflow; SF, shallow baseflow; BF, deeper baseflow. Horizontal lines represent the baseline median concentrations. The difference between TDP and TFP_{coll} is TP_{coll}, the difference between DRP and FRP_{coll} is RP_{coll} and the difference between DUP and FUP_{coll} is UP_{coll}.

mobilised with a larger first source (Fig. 9) (Evans and Davies, 1998; House and Warwick, 1998).

During A-1, shallow GW P was dominantly FRP_{coll} (Fig. 6) and concentrations were stable during the event. In the stream, P was mostly FRP_{coll} and to a lesser extent TUP and FUP_{coll}, especially during QF and IF where concentrations were higher (Fig. 6, Fig. 11). During the event, 94 % of the flow occurred as BF that transferred most of the P load as FRP_{coll} (0.025 g ha^{-1}) (Fig. 8). The C-Q hysteresis showed that the unique source of P was easily mobilised or proximal (Fig. 9) (Evans and Davies, 1998; House and Warwick, 1998).

4. Discussion

The analysis of water quality data from multiple hillslope locations revealed contrasting baseline P concentrations, fractions and species between the two catchments with different dominating soil chemistry and land use. Contrasts were also revealed during high flow events of different magnitudes and timing of the year that may be due to dominant hydrological flow pathways mobilising different P sources.

4.1. Influences of catchment characteristics on colloidal phosphorus

Monitoring of P fractions during baseflow conditions showed that fine (<200 nm) P is an important component of stream TP as reported elsewhere (Gottselig et al., 2014; Gu et al., 2020). However, the results also indicated a limited presence of medium-sized colloidal P species both at baseline and in storm samples in all parts of the hillslope to stream continuum. This finding was constantly observed despite contrasting SMD, land use, storm sizes and stream outlet nutrient fluxes. Some further interpretation is provided about other parameters measured in the samples (**Table C**) and relationships with larger particulates and finer fractions.

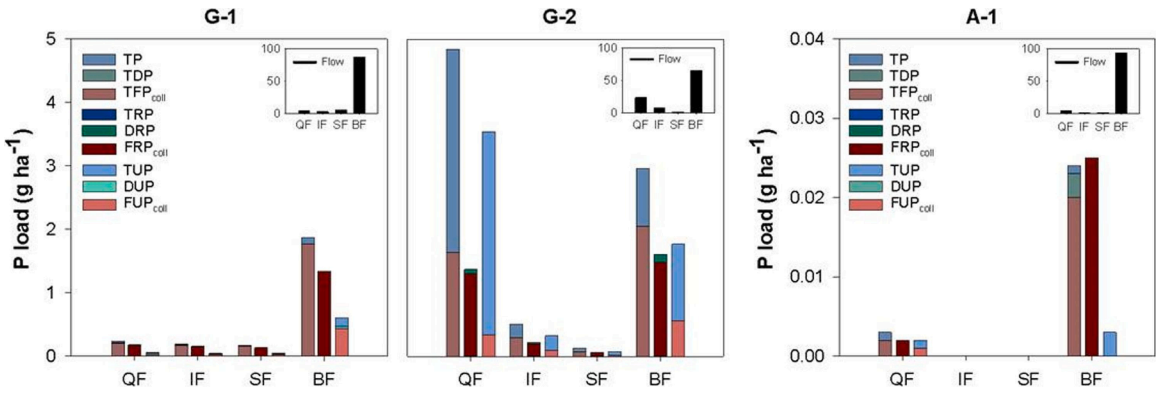

Fig. 8. Stream phosphorus loads during quickflow QF, interflow IF, shallow baseflow SF, deeper baseflow BF during flow events G-1, G-2 and A-1. Fine P (red) is included in dissolved P (green) which is included in total P (blue). Stream flow expressed as percentage of event total flow. The difference between TDP and TFP_{coll} is TP_{coll}, the difference between DRP and FRP_{coll} is RP_{coll} and the difference between DUP and FUP_{coll} is UP_{coll}. (For interpretation of the references to colour in this figure legend, the reader is referred to the web version of this article.)

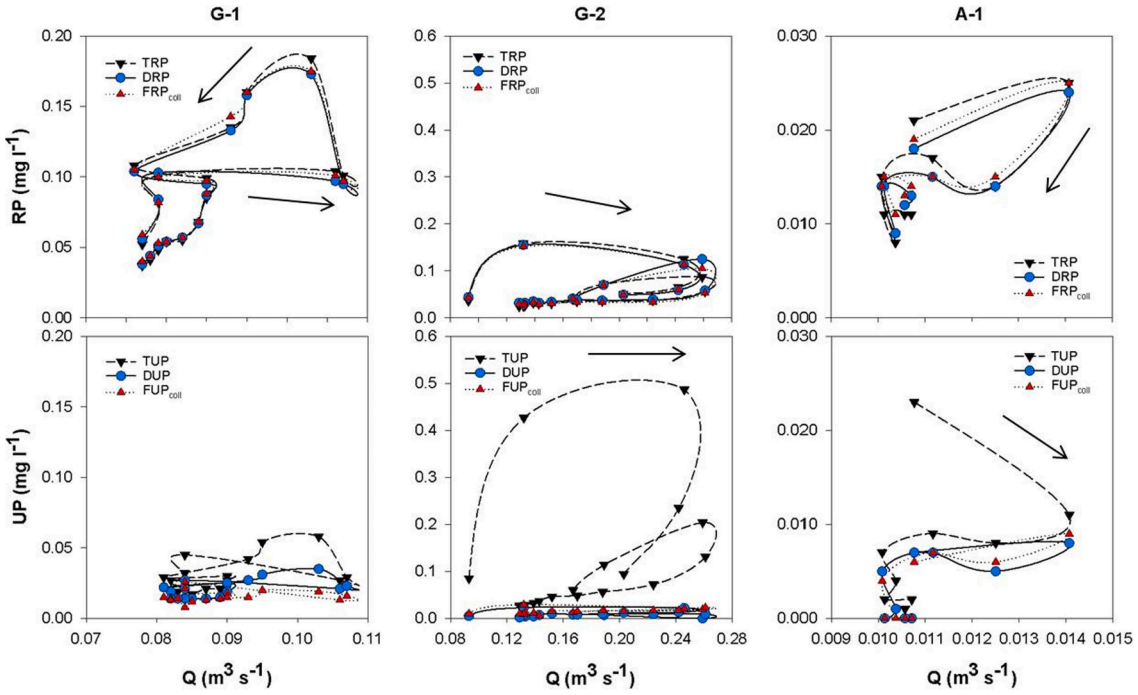

Fig. 9. Concentration-discharge hysteresis for flow events G-1, G-2 and A-1. Reactive and unreactive P (in the total, dissolved and fine P fractions) are shown at the top and bottom, respectively. The difference between TDP and TFP_{coll} is TP_{coll}, the difference between DRP and FRP_{coll} is RP_{coll} and the difference between DUP and FUP_{coll} is UP_{coll}.

For example, higher TP and Fe concentrations measured in TG (particularly in shallow GW at TG-DS) (**Table C**) may indicate that P is associated with Fe in larger (>450 nm) colloidal P complexes. Coarse colloids are mostly composed of Fe hydroxyphosphate minerals and Fe oxyhydroxides (Baken et al., 2016a) and, although recent colloidal P studies have focused on streams, this is also in agreement with the recurrent observation that stream P is related to colloidal Fe (Gottselig et al., 2014; Baken et al., 2016b; van der Grift et al., 2018). Moreover, concentrations in total OC measured in soil solution and shallow GW (**Table C**) suggest the presence of highly mobile Fe-OM associations in TG. Measurements of shallow GW ORP and NO_3^--N concentrations (**Table C**) revealed specific geochemical processes, similarly observed by McAleer et al. (2017), which suggests that these Fe-P complexes originate from the soil, where similar P forms were observed, or from upslope. Contrary, fine (<200 nm) P may be dominant as an association of P with OM and amorphous Fe(Al) oxides in nano-particles in TA, as observed by Jiang et al. (2015). These differences in P binding forms (e.g. humic-Al(and Fe) association, Fe(hydr)oxides and clay minerals) between TG and TA can result in different reactivity and solubility of colloidal P complexes (Beauchemin et al., 2003; Liu et al., 2014) with a lower reactivity of P bound to Fe complexes, as shown by others (Ilg et al., 2008; Toor et al., 2003; Weng et al., 2011).

Moreover, soil physical properties (e.g macroporosity) facilitating water flow in TG compared to TA (not presented here) may limit P attenuation processes by allowing stable forms of P to bypass the soil matrix *via* preferential flow. This can play a significant role in PP delivery to subsurface P loading (Nazari et al., 2020), and facilitate colloidal P transport (Bol et al., 2016; Julich et al., 2017) and leaching to GW (Ilg et al., 2008; Mayer and Jarrell, 1995).

Similarly, lower shallow bedrock saturated hydraulic conductivity (K_{sat}) in TG compared to TA (Table 1) may facilitate shallow GW P attenuation/transformation processes before its delivery to the stream

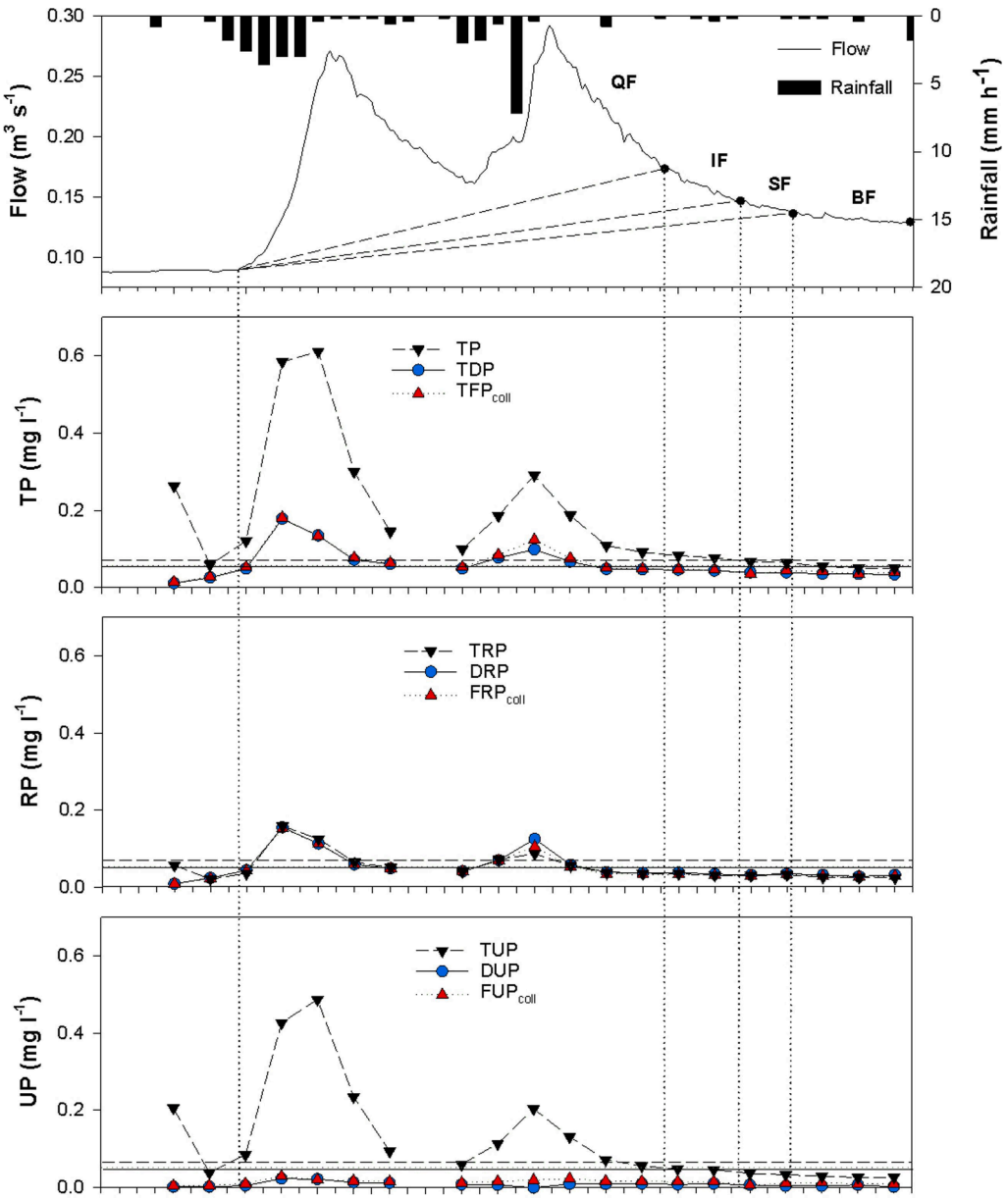

Fig. 10. Total P, reactive P and unreactive P (in the total, dissolved and fine P fractions) transfer pathways based on hydrograph recession analysis for flow event G-2. QF, quickflow; IF, interflow; SF, shallow baseflow; BF, deeper baseflow. Horizontal lines represent the baseline median concentrations. The difference between TDP and TFP_{coll} is TP_{coll}, the difference between DRP and FRP_{coll} is RP_{coll} and the difference between DUP and FUP_{coll} is UP_{coll}.

leading to the geochemical heterogeneity observed between shallow GW at TG-DS and TG-stream, in agreement with McAleer et al. (2017). Contrary in TA, the higher shallow bedrock K_{sat} (Table 1) and the subsequent limitation of geochemical processes may explain the geochemical homogeneity observed.

The results from these baseflow monitoring campaigns suggest that soil and bedrock controls influence the below-ground delivery of colloidal P to the stream. The dominant P fractions in both soil water, GW and stream water may therefore differ within the landscape (Gottselig et al., 2020). For example, P fractions in OM-richer soils landscapes may differ from the particulate and fine P fractions mainly observed in this study. High permeability soils and landscapes (such as karst landscapes, for example) may lead to similar P fractions in soil water, GW and stream water, while lower permeability soils may result in more heterogeneity. To better support this, investigations of P fractions in other chemical and physical settings are required. To further refine process understanding of colloidal P delivery to stream water, monitoring should also include the particulate and fine P fractions (Gottselig et al., 2014; Gu et al., 2020).

4.2. *Influences of storm event characteristics on colloidal phosphorus*

Monitoring of P fractions during high flow events showed that during both events in TG, shallow GW delivered similar P fractions to the stream most likely due to similar GW redox conditions (revealed by ORP and NO_3^--N measurements – **Table D**). High GW Fe concentrations (**Table D**) and associated stream P and Fe peaks suggest that GW P is associated to Fe, a common association in the coarse colloidal fraction (Baken et al., 2016a). During these events, results suggested that GW P was delivered to the stream 5 (G-1) to 17 (G-2) hours after the flow started to rise. Similar to baseflow conditions, the low sandstone bedrock K_s (Table 1) may facilitate the attenuation/transformation of P-Fe associations before their delivery to the stream by promoting denitrifying conditions in shallow GW (**Table D**). Hence, the fine P fraction

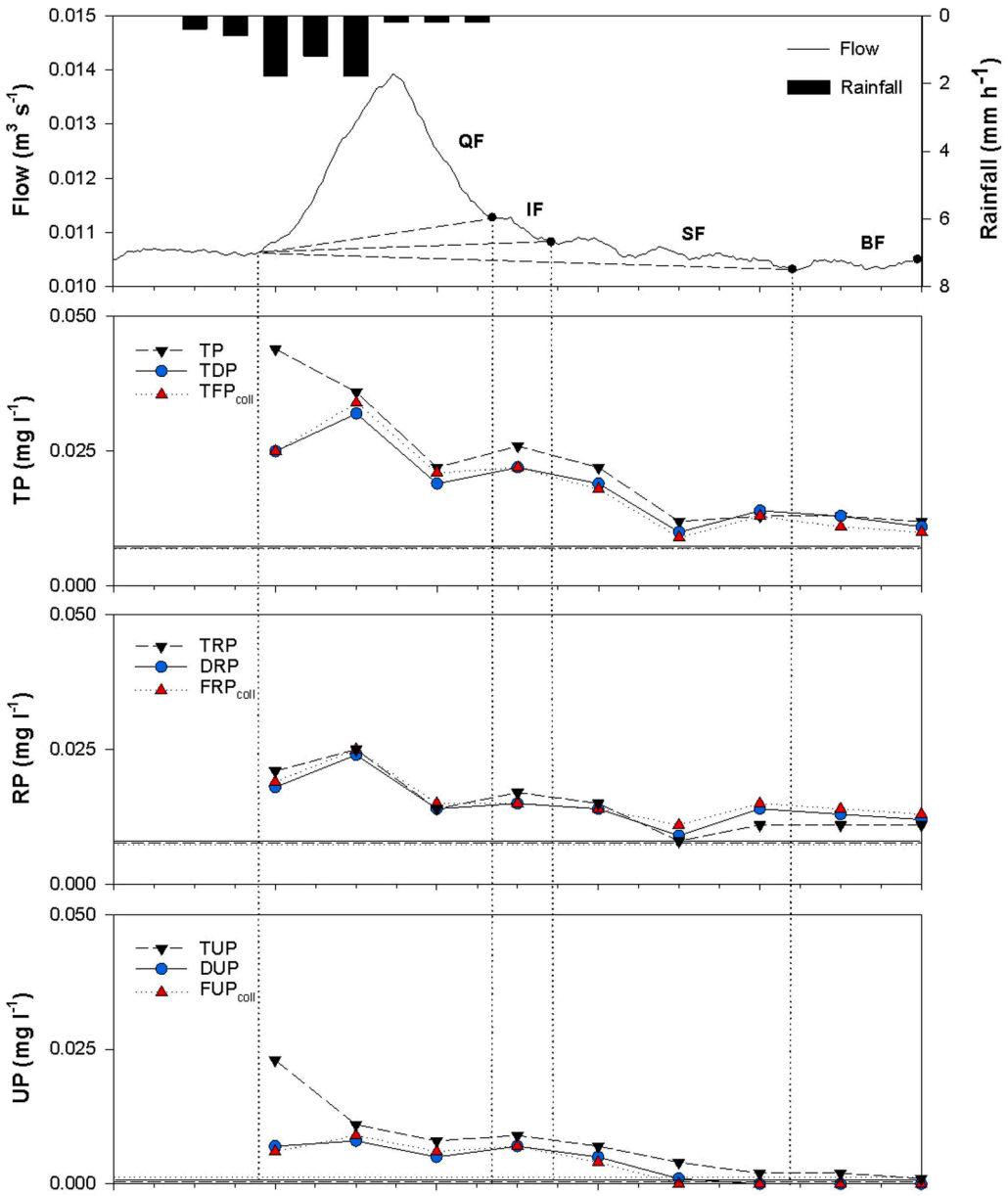

Fig. 11. Total P, reactive P and unreactive P (in the total, dissolved and fine P fractions) transfer pathways based on hydrograph recession analysis for flow event A-1. QF, quickflow; IF, interflow; SF, shallow baseflow; BF, deeper baseflow. Horizontal lines represent the baseline median concentrations. The difference between TDP and TFP_{coll} is TP_{coll}, the difference between DRP and FRP_{coll} is RP_{coll} and the difference between DUP and FUP_{coll} is UP_{coll}.

was dominant in the stream during G-1 (85–96 % of TP) even though it was not dominant in GW, independently of the rainfall event (19–21 % of TP). However, the high P load transferred *via* the QF pathway during G-2 may explain the dominance of TUP in stream during this event. This is in agreement with Heathwaite and Johnes (1996) who found that PP represented a significant P fraction in surface runoff and confirmed by Van Esbroeck et al. (2017) who showed an increase in PP concentrations, particularly in surface runoff, with rainfall. Investigation of the larger colloidal fractions would be needed to show their role as P-carriers, as PP represented 79 to 81 % of shallow GW TP and 44 to 68 % of stream TP during G-2.

During A-1 in TA, results suggested that GW P was delivered more quickly to the stream than in TG (2 h after the flow started to rise) due to the higher shallow bedrock K_s (Table 1). The fine P fraction had an important role in-stream (80 to 100 % of TP) due to its dominance in GW (99 % of TP), the principal contributor of the stream flow. However, PP contribution to the stream increased when the hydrological flowpath tended towards more surface water connecting more land (Fig. 6). This suggests that during an event with more QF pathway PP, which includes larger colloids, may be dominant and particularly in winter when many arable fields are bare (e.g., Van Esbroeck et al., 2017).

The results from these storm event monitoring campaigns suggest various controlling factors on the below-ground delivery of colloidal P. The hydrological flow pathway and the subsequent mobilised P sources influence the P fractions delivered to the stream, in agreement with Van Esbroeck et al. (2017). This suggests that the increasing intensity of rainfall events may result in an increasing overland contribution of the coarser colloids in P delivery, independently of the landscapes chemical and physical settings. The temporal dynamics of colloids have previously been linked to water flux (Gottselig et al., 2020). Contrary, smaller events may increase the importance of site-specific soil and bedrock controls on colloidal P delivery. However, further monitoring campaigns would be needed at the field scale for both stream and GW to cover a wider range of high flow conditions. This is especially important in Fe-

rich catchments (Baken et al., 2016b; Gottselig et al., 2014; van der Grift et al., 2018) but other landscapes settings should also be considered. This should be carried out outside and during the 'closed period' when fertilizer application is prohibited to better assess the effect of agricultural P sources. This would also help to better constrain the controlling factors on medium-sized colloidal P in space and time. A higher sampling frequency (<2 h) may resolve P concentrations and loads when short concentrations peaks are observed (e.g. during G-2) that may be prone to underestimation. The GW sampling setup may also need further refinement to better quantify the accuracy and precision of this system and especially with regard to the particulate fraction.

Concurrent to the below-ground sources, stream colloidal P concentrations can also result from the mobilisation of fine P-bearing sediments of the stream bed which can have a strong influence on baseflow P concentrations (McDowell et al., 2020). The net transport of these colloids can be strongly controlled by background water chemistry (Ren and Packman, 2002). Moreover, sediment yield rate can significantly influence colloidal P loss in runoff during rainfall events (He et al., 2019).

5. Conclusions

In addition to total and dissolved P fractions, this study investigated medium-sized colloidal (200–450 nm) and fine (<200 nm; fine colloidal, nano-particulate and truly dissolved) P fractions in soil solution, shallow GW and in streams along two agricultural hillslope transects to assess the importance of below-ground colloidal P (and other fractions) delivery. The study suggested an effect of catchment characteristics (soil chemistry) on soil solution and shallow GW baseline P fractions. Fine P was dominant in the Al-rich Arable transect whereas PP, and possibly larger colloidal P (450–1000 nm) forms, was dominant in the Fe-rich Grassland transect. In both transects, fine P was dominant in the stream. The study indicated a limited presence of medium-sized colloidal P species. Smaller and less intense flow events facilitated below-ground P delivery (either in the fine or larger colloidal fractions) whereas a more intense flow event led to more overland flow mobilising PP and possibly larger colloidal sources which can vary through the year (closed period).

The experimental set-up in this study from hillslope to stream has revealed a predominant coarse and fine colloidal mobilisation and delivery system and can be used to look deeper into these fractions and species. As well as larger and unreactive fractions, colloids therefore play an important role in the P delivery to streams and require further investigation at the field-scale for different physical and chemical settings and hydro-climatic conditions.

Declaration of Competing Interest

The authors declare that they have no known competing financial interests or personal relationships that could have appeared to influence the work reported in this paper.

Acknowledgements

We thank the ACP landowners and farmers for their support, field access and fencing permission, the ACP staff David Ryan, Oisín Coakley and Mark Boland for advices, assistance in field setup, sampling, data downloads, and for providing the fertilisation data, Una Cullen for providing the meteorological data and Simon Leach for creating the GIS maps. The laboratory support of Denis Brenan and Maria Radford for water samples analysis is greatly appreciated. The authors also thank the farm staff of Johnstown Castle and John Murphy for help with the GW sampler, Gérard Gruau and Sen Gu from Géosciences Rennes for advice on the soil water traps. Funding was provided by the Department of Agriculture, Food and the Marine through the Teagasc ACP and by the Teagasc Walsh Fellowship Programme.

Appendix A. Supplementary material

Supplementary data to this article can be found online at https://doi.org/10.1016/j.catena.2021.105735.

References

Anderson, A.E., Weiler, M., Alila, Y., Hudson, O., 2009. Dye staining and excavation of a lateral preferential flow network. Hydrol. Earth Syst. Sci. 13, 935–944.

Archbold, M., Bruen, M., Deakin, J., Doody, D., Flynn, R., Kelly-Quinn, M. et al., 2010. Contaminant movement and attenuation along pathways from the land surface to aquatic receptors – A review. Strive Research Report 2007-WQ-CD-1-S1, 1-177.

Askew, F.E., 2005. Persulfate method for simultaneous determination of total nitrogen and total phosphorus. 4500–P J, in: Eaton, A.D., Clesceri, L.S., Rice, W.E., Greenberg, A.E. (Eds.), Standard Methods for the Examination of Water and Wastewater, 21st edition. ISBN 0-87553-047-8. American Public Health Association, 800 1 street, NW Washington, DC 2001-3710, pp. 160-161.

Askew, F.E., Smith, R.K., 2005a. Inorganic non metallic constituents; Phosphorus; Method 4500-P F. Automated ascorbic acid reduction method, in: Eaton, D.A., Clesceri, L.S., Rice, E.W., Greensberg, A.E. (Eds.), Standard Methods for the Examination of Waters and Waste Water, 21st edition. ISBN 0-87553-047-8. American Public Health Association, 800 1 street, NW Washington, DC 2001-3710, pp. 4-155.

Askew, F.E., Smith, R.K., 2005b. Inorganic non metallic constituents; Method 4500-NO3-H. Automated Hydrazine Reduction method, in: Eaton, D.A., Clesceri, L.S., Rice, E.W., Greensberg, A.E. (Eds.), Standard Methods for the Examination of Waters and Waste Water, 21st edition. ISBN 0-87553-047-8. American Public Health Association, 800 1 street, NW Washington, DC 2001-3710, pp. 4-125.

Askew, F.E., Smith, R.K., 2005c. Inorganic non metallic constituents; Method 4500-NO2-Nitrogen (Nitrite), in: Eaton, D.A., Clesceri, L.S., Rice, E.W., Greensberg, A.E. (Eds.), Standard Methods for the Examination of Waters and Waste Water, 21st edition. ISBN 0-87553-047-8. American Public Health Association, 800 1 street, NW Washington, DC 2001-3710.

Bachmair, S., Weiler, M., 2012. Hillslope characteristics as controls of subsurface flow variability. Hydrology and Earth System Sciences 16, 3699–3715. https://doi.org/10.5194/hess-16-3699-2012.

Bachmair, S., Weiler, M., Troch, P.A., 2012. Intercomparing hillslope hydrological dynamics: spatio–temporal variability and vegetation cover effects. Water Resources Research 48 (5). https://doi.org/10.1029/2011WR011196.

Baird, R.B., 2005. Aggregate organic constituents; Total Organic Carbon (TOC)/Method 5310 B High temperature combustion methods, in: Eaton, D.A., Clesceri, L.S., Rice, E.W., Greensberg, A.E. (Eds.). Standard Methods for the Examination of Waters and Waste Water, 21st edition. ISBN 0-87553-047-8. American Public Health Association, 800 1 street, NW Washington, DC 2001-3710, pp. 5-21.

Baken, S., Moens, C., van der Grift, B., Smolders, E., 2016a. Phosphate binding by natural iron-rich colloids in streams. Water Res. 98, 326–333. https://doi.org/10.1016/j.watres.2016.04.032.

Baken, S., Regelink, I.C., Comans, R.N.J., Smolders, E., Koopmans, G.F., 2016b. Iron-rich colloids as carriers of phosphorus in streams: A field-flow fractionation study. Water Res. 99, 83–90. https://doi:10.1016b/j.watres.2016.04.060.

Beauchemin, S., Hesterberg, D., Chou, J., Beauchemin, M., Simard, R.R., Sayers, D.E., 2003. Speciation of phosphorus in phosphorus-enriched agricultural soils using X-ray absorption near-edge structure spectroscopy and chemical fractionation. J Environ Qual 32 (5), 1809–1819. https://doi.org/10.2134/jeq2003.1809.

Bender, M.A., dos Santos, D.R., Tiecher, T., Minella, J.P.G., de Barros, C.A.P., Ramon, R., 2018. Phosphorus dynamics during storm events in a subtropical rural catchment in southern Brazil. Agric, Ecosyst Environ 261, 93–102. https://doi.org/10.1016/j.agee.2018.04.004.

Bieroza, M., Heathwaite, A.L., 2015. Seasonal variation in phosphorus concentration–discharge hysteresis inferred from high-frequency *in situ* monitoring. J. Hydrol. 524, 333–347. https://doi.org/10.1016/j.jhydrol.2015.02.036.

Bol, R., Julich, D., Brödlin, D., Siemens, J., Kaiser, K., Dippold, M.A., Spielvogel, S., Zilla, T., Mewes, D., von Blanckenburg, F., Puhlmann, H., Holzmann, S., Weiler, M., Amelung, W., Lang, F., Kuzyakov, Y., Feger, K.-H., Gottselig, N., Klumpp, E., Missong, A., Winkelmann, C., Uhlig, D., Sohrt, J., von Wilpert, K., Wu, B., Hagedorn, F., 2016. Dissolved and colloidal phosphorus fluxes in forest ecosystems—an almost blind spot in ecosystem research. J Plant Nutr Soil Sci 179 (4), 425–438.

Cook, R.D., 1979. Influential Observations in Linear Regression. J. Am. Stat. Assoc. 74, 169–174. https://doi.org/10.1080/01621459.1979.10481634.

Cordell, D., White, S., 2014. Life's Bottleneck: Sustaining the World's Phosphorus for a Food Secure Future. Annu. Rev. Environ. Resour. 39, 161. https://doi.org/10.1146/annurev-environ-010213-113300.

Doody, D.G., Archbold, M., Foy, R.H., Flynn, R., 2012. Approaches to the implementation of the Water Framework Directive: Targeting mitigation measures at critical source areas of diffuse phosphorus in Irish catchments. J. Environ Manage. 93 (1), 225. https://doi.org/10.1016/j.jenvman.2011.09.002.

Duan, J., Jang, J., Tang, C., Chen, L., Liu, Y., Wang, L., 2017. Effects of rainfall patterns and land cover on the subsurface flow generation of sloping Ferralsols in southern China. PLoS One 12 (8). https://doi.org/10.1371/journal.pone.0182706.

Dupas, R., Gruau, G., Gu, S., Humbert, G., Jaffrézic, A., Gascuel-Odoux, C., 2015. Groundwater control of biogeochemical processes causing phosphorus release from riparian wetlands. Water Res. 84, 307–314. https://doi.org/10.1016/j.watres.2015.07.048.

Evans, C., Davies, T.D., 1998. Causes of concentration/discharge hysteresis and its potential as a tool for analysis of episode hydrochemistry. Water Resour Res 34, 129–137. https://doi.org/10.1029/97WR01881.
Fealy, R.M., Buckley, C., Mechan, S., Melland, A., Mellander, P-E., Shortle, G., et al., 2010. The Irish Agricultural Catchments Programme: catchment selection using spatial multi-criteria decision analysis. Soil Use Manage 26, 225–236. https://doi.org/10.1111/j.1475-2743.2010.00291.x.
Fresne, M., Jordan, P., Fenton, O., Mellander, P.-E., Daly, K., 2021. Soil chemical and fertilizer influences on soluble and medium-sized colloidal phosphorus in agricultural soils. Sci. Total Environ. 754, 142112. https://doi.org/10.1016/j.scitotenv.2020.142112.
Gottler, R.A., Piwoni, M.D., 2005. Metals; Method 3120 B. Inductively coupled plasma (ICP) method, in: Eaton, D.A., Clesceri, L.S., Rice, E.W., Greensberg, A.E. (Eds.), Standard Methods for the Examination of Waters and Waste Water, 21st edition. American Public Health Association, 800 1 street, NW Washington, DC 2001-3710, pp. 3-39.
Gottselig, N., Bol, R., Nischwitz, V., Vereecken, H., Amelung, W., Klumpp, E., 2014. Distribution of Phosphorus-Containing Fine Colloids and Nanoparticles in Stream Water of a Forest Catchment. Vadose Zone J. 13 (7), 1–11. https://doi.org/10.2136/vzj2014.01.0005.
Gottselig, N., Sohrt, J., Uhlig, D., Nischwitz, V., Weiler, M., Amelung, W., 2020. Groundwater controls on colloidal transport in forest stream waters. Sci. Total Environ. 717, 134638. https://doi.org/10.1016/j.scitotenv.2019.134638.
Graham, C.B., Woods, R.A., McDonnell, J.J., 2010. Hillslope threshold response to rainfall: (1) A field based forensic approach. J. Hydrol. 393, 65–76. https://doi.org/10.1016/j.jhydrol.2009.12.015.
Gu, S., Gruau, G., Dupas, R., Jeanneau, L., 2020. Evidence of colloids as important phosphorus carriers in natural soil and stream waters in an agricultural catchment. J Environ Qual 49 (4), 921–932. https://doi.org/10.1002/jeq2.20090.
He, X., Zheng, Z., Li, T., He, S., Zhang, X., Wang, Y., Huang, H., Yu, H., Liu, T., Lin, C., 2019. Transport of colloidal phosphorus in runoff and sediment on sloping farmland in the purple soil area of south-western China. Environ Sci Pollut Res 26 (23), 24088–24098. https://doi.org/10.1007/s11356-019-05735-5.
Heathwaite, A.L., Johnes, P.J., 1996. Contribution of nitrogen species and phosphorus fractions to stream water quality in agricultural catchments. Hydrol Process 10, 971–983. https://doi.org/10.1002/(SICI)1099-1085(199607)10:7<971::AID-HYP351>3.0.CO;2-N.
Heathwaite, L., Haygarth, P., Matthews, R., Preedy, N., Butler, P., 2005. Evaluating colloidal phosphorus delivery to surface waters from diffuse agricultural sources. J Environ Qual 34, 287–298. https://doi.org/10.2134/jeq2005.0287a.
Henderson, R., Kabengi, N., Mantripragada, N., Cabrera, M., Hassan, S., Thompson, A., 2012. Anoxia-Induced Release of Colloid- and Nanoparticle-Bound Phosphorus in Grassland Soils. Environ Sci Technol 46, 11727–11734. https://doi.org/10.1021/es302395r.
Holman, I.P., Whelan, M.J., Howden, N.J.K., Bellamy, P.H., Willby, N.J., Rivas-Casado, M., McConvey, P., 2008. Phosphorus in groundwater—an overlooked contributor to eutrophication? Hydrol. Process. 22, 5121–5127. https://doi.org/10.1002/hyp.7198.
House, W.A., Warwick, M.S., 1998. Hysteresis of the solute concentration/discharge relationship in rivers during storms. Water Res 32, 2279–2290. https://doi.org/10.1016/S0043-1354(97)00473-9.
Ilg, K., Dominik, P., Kaupenjohann, M., Siemens, J., 2008. Phosphorus-induced mobilization of colloids: model systems and soils. Eur J Soil Sci 59, 233–246. https://doi.org/10.1111/j.1365-2389.2007.00982.x.
Jiang, X., Bol, R., Nischwitz, V., Siebers, N., Willbold, S., Vereecken, H., Amelung, W., Klumpp, E., 2015. Phosphorus Containing Water Dispersible Nanoparticles in Arable Soil. J. Environ. Qual. 44 (6), 1772–1781. https://doi.org/10.2134/jeq2015.02.0085.
Jiang, C., Sequaris, J., Vereecken, H., Klumpp, E., 2013. Diffusion-controlled mobilization of water-dispersible colloids from three German silt loam topsoils: effect of temperature. Eur J Soil Sci 64, 777–786. https://doi.org/10.1111/ejss.12086.
Julich, D., Julich, S., Feger, K., 2017. Phosphorus fractions in preferential flow pathways and soil matrix in hillslope soils in the Thuringian Forest (Central Germany). J Plant Nutr Soil Sci 180, 407–417. https://doi.org/10.1002/jpln.201600305.
Lehmann, P., Hinz, C., McGrath, G., Tromp-van-Meerveld, H.J., McDonnell, J.J., 2007. Rainfall threshold for hillslope outflow: an emergent property of flow pathway connectivity. Hydrol. Earth Syst. Sci. 11, 1047–1063. https://doi.org/10.5194/hess-11-1047-2007.
Liu, J., Yang, J., Liang, X., Zhao, Y., Cade-Menun, B., Hu, Y., 2014. Molecular Speciation of Phosphorus Present in Readily Dispersible Colloids from Agricultural Soils. Soil Sci. Soc. Am. J. 78, 47–53. https://doi.org/10.2136/sssaj2013.05.0159.
Lookman, R., Vandeweert, N., Merckx, R., Vlassak, K., 1995. Geostatistical assessment of the regional distribution of phosphate sorption capacity parameters (FeOX and AlOX) in northern Belgium. Geoderma 66, 285–296. https://doi.org/10.1016/0016-7061(94)00084-N.
Mabilde, L., De Neve, S., Sleutel, S., 2017. Regional analysis of groundwater phosphate concentrations under acidic sandy soils: Edaphic factors and water table strongly mediate the soil P-groundwater P relation. J. Environ. Manage. 203, 429–438. https://doi.org/10.1016/j.jenvman.2017.07.058.
Mayer, T.D., Jarrell, W.M., 1995. Assessing Colloidal Forms of Phosphorus and Iron in the Tualatin River Basin. J. Environ. Qual. 24, 1117–1124. https://doi.org/10.2134/jeq1995.00472425002400060010x.
McAleer, E.B., Coxon, C.E., Richards, K.G., Jahangir, M.M.R., Grant, J., Mellander, P.-E., 2017. Groundwater nitrate reduction versus dissolved gas production: A tale of two catchments. Sci. Total Environ. 586, 372–389. https://doi.org/10.1016/j.scitotenv.2016.11.083.
McDowell, R.W., Cox, N., Daughney, C.J., Wheeler, D., Moreau, M., 2015. A National Assessment of the Potential Linkage between Soil, and Surface and Groundwater Concentrations of Phosphorus. J. Am. Water Resour. Assoc. 51 (4), 992–1002. https://doi.org/10.1111/1752-1688.12337.
McDowell, R.W., Depree, C., Stenger, R., 2020. Likely controls on dissolved reactive phosphorus concentrations in baseflow of an agricultural stream. J Soils Sediments 20, 3254–3265. https://doi.org/10.1007/s11368-020-02644-w.
McGinley, P.M., Masarik, K.C., Gotkowitz, M.B., Mechenich, D.J., 2016. Impact of anthropogenic geochemical change and aquifer geology on groundwater phosphorus concentrations. Appl. Geochem. 72, 1–9. https://doi.org/10.1016/j.apgeochem.2016.05.020.
Mellander, P.-E., Jordan, P., Shore, M., McDonald, N.T., Wall, D.P., Shortle, G., et al., 2016. Identifying contrasting influences and surface water signals for specific groundwater phosphorus vulnerability. Sci. Total Environ. 541, 292–302. https://doi.org/10.1016/j.scitotenv.2015.09.082.
Mellander, P.-E., Melland, A., Murphy, P.N.C., Wall, D.P., Shortle, G., Jordan, P., 2014. Coupling of surface water and groundwater nitrate-N dynamics in two permeable agricultural catchments. J. Agric. Sci. 152, S107–S124. https://doi.org/10.1017/S0021859614000021.
Mellander, P.-E., Melland, A.R., Jordan, P., Wall, D.P., Murphy, P.N.C., Shortle, G., 2012. Quantifying nutrient transfer pathways in agricultural catchments using high temporal resolution data. Environ Sci & Policy 24, 44–57. https://doi.org/10.1016/j.envsci.2012.06.004.
Missong, A., Bol, R., Nischwitz, V., Krüger, J., Lang, F., Siemens, J., Klumpp, E., 2018. Phosphorus in water dispersible-colloids of forest soil profiles. Plant Soil 427 (1-2), 71–86.
Mohanty, S.K., Saiers, J.E., Ryan, J.N., 2015. Colloid Mobilization in a Fractured Soil during Dry-Wet Cycles: Role of Drying Duration and Flow Path Permeability. Environ Sci Technol 49, 9100–9106. https://doi.org/10.1021/acs.est.5b00889.
Moloney, T., Fenton, O., Daly, K., 2020. Ranking connectivity risk for phosphorus loss along agricultural drainage ditches. Sci. Total Environ. 703, 134556 https://doi.org/10.1016/j.scitotenv.2019.134556.
Montalvo, D., Degryse, F., McLaughlin, M.J., 2015. Natural Colloidal P and Its Contribution to Plant P Uptake. Environ Sci Technol 49 (6), 3427–3434. https://doi.org/10.1021/es504643f.
Nazari, S., Ford, W.I., King, K.W., 2020. Impacts of preferential flow and agroecosystem management on subsurface particulate phosphorus loadings in tile-drained landscapes. J Environ Qual 49 (5), 1370–1383. https://doi.org/10.1002/jeq2.20116.
Neidhardt, H., Schoeckle, D., Schleinitz, A., Eiche, E., Berner, Z., Tram, P.T.K., Lan, V.M., Viet, P.H., Biswas, A., Majumder, S., Chatterjee, D., Oelmann, Y., Berg, M., 2018. Biogeochemical phosphorus cycling in groundwater ecosystems – Insights from South and Southeast Asian floodplain and delta aquifers. Sci Total Environ 644, 1357–1370. https://doi.org/10.1016/j.scitotenv.2018.07.056.
Ren, J., Packman, A.I., 2002. Effects of Background Water Composition on Stream-Subsurface Exchange of Submicron Colloids. J. Environ. Eng. 128 (7), 624–634. https://doi.org/10.1061/(ASCE)0733-9372(2002)128:7(624).
Schelde, K., de Jonge, L.W., Kjaergaard, C., Laegdsmand, M., Rubæk, G.H., 2006. Effects of Manure Application and Plowing on Transport of Colloids and Phosphorus to Tile Drains. Vadose Zone J. 5, 445–458. https://doi.org/10.2136/vzj2005.0051.
Schilling, K.E., Kim, S., Jones, C.S., Wolter, C.F., 2017. Orthophosphorus Contributions to Total Phosphorus Concentrations and Loads in Iowa Agricultural Watersheds. J Environ Qual 46, 828–835. https://doi.org/10.2134/jeq2017.01.0015.
Schoumans, O.F., Chardon, J.W., Bechmann, M.E., Gascuel-Odoux, C., Hofman, G., Kronvang, B., Rubæk, G.H., Ulén, B., Doriozh, J.-M., 2014. Mitigation options to reduce phosphorus losses from the agricultural sector and improve surface water quality: A review. Sci Total Environ 468–469, 1255–1266. https://doi.org/10.1016/j.scitotenv.2013.08.061.
Schulte, R.P.O., Diamond, J., Finkele, K., Holden, N.M., Brereton, A.J., 2005. Predicting the soil moisture conditions of Irish grassland. Irish Journal of Agriculture and Food Research 44 (1), 95–110.
Sharpley, A., Foy, B., Withers, P., 2000. Practical and Innovative Measures for the Control of Agricultural Phosphorus Losses to Water: An Overview. J Environ Qual 29 (1), 1–9. https://doi.org/10.2134/jeq2000.00472425002900010001x.
Shore, M., Murphy, S., Mellander, P.-E., Shortle, G., Melland, A.R., Crockford, L., O'Flaherty, V., Williams, L., Morgan, G., Jordan, P., 2017. Influence of stormflow and baseflow phosphorus pressures on stream ecology in agricultural catchments. Sci Total Environ 590-591, 469–483. https://doi.org/10.1016/j.scitotenv.2017.02.100.
Siemens, J., Ilg, K., Lang, F., Kaupenjohann, M., 2004. Adsorption controls mobilization of colloids and leaching of dissolved phosphorus. Eur J Soil Sci 55, 253–263. https://doi.org/10.1046/j.1365-2389.2004.00596.x.
Sinha, E., Michalak, A.M., Balaji, V., 2017. Eutrophication will increase during the 21st century as a result of precipitation changes. Science 357, 407–408. https://doi.org/10.1126/science.aan2409.
Toor, G.S., Condron, L.M., Di, H.J., Cameron, K.C., Cade-Menun, B.J., 2003. Characterization of organic phosphorus in leachate from a grassland soil. Soil Biol Biochem 35, 1317–1323. https://doi.org/10.1016/S0038-0717(03)00202-5.
Tromp-van Meerveld, H.J., Weiler, M., 2008. Hillslope dynamics, modeled with increasing complexity. J. Hydrol. 361, 24–40. https://doi.org/10.1016/j.jhydrol.2008.07.019.
van der Grift, B., Osté, L., Schot, P., Kratz, A., van Popta, E., Wassen, M., et al., 2018. Forms of phosphorus in suspended particulate matter in agriculture-dominated lowland catchments: Iron as phosphorus carrier. Sci. Total Environ. 631–632, 115–129. https://doi.org/10.1016/j.scitotenv.2018.02.266.

Van Esbroeck, C.J., Macrae, M.L., Brunke, R.R., McKague, K., 2017. Surface and subsurface phosphorus export from agricultural fields during peak flow events over the nongrowing season in regions with cool, temperate climates. J. Soil Water Conserv. 72 (1), 65–76. https://doi.org/10.2489/jswc.72.1.65.

Wall, D.P., Murphy, P.N.C., Melland, A.R., Mechan, S., Shine, O., Buckley, C., et al., 2012. Evaluating nutrient source regulations at different scales in five agricultural catchments. Environ Sci Policy 24, 34–43. https://doi.org/10.1016/j.envsci.2012.06.007.

Weng, L., Vega, F.A., van Riemsdijk, W.H., 2011. Competitive and Synergistic Effects in pH Dependent Phosphate Adsorption in Soils: LCD Modeling. Environ Sci Technol 45, 8420–8428. https://doi.org/10.1021/es201844d.

Withers, P.J.A., Neal, C., Jarvie, H.P., Doody, D.G., 2014. Agriculture and Eutrophication: Where Do We Go from Here? Sustainability 6, 5853–5875. https://doi.org/10.3390/su6095853.